Available online at www.sciencedirect.com

ScienceDirect

journal homepage: http://www.elsevier.com/locate/acme

Original Research Article

Experimental research of cable tension tuning of a scaled model of cable stayed bridge

W. Pakos *, *Z. Wójcicki*, *J. Grosel*, *K. Majcher*, *W. Sawicki*

Wrocław University of Technology, Wybrzeże Wyspiańskiego 27, 50-370 Wrocław, Poland

ARTICLE INFO

Article history:
Received 3 December 2014
Accepted 1 September 2015
Available online 17 October 2015

Keywords:
Cable-stayed footbridge
Vibration reduction
Experimental research
Model-based testing
Modal analysis

ABSTRACT

The paper describes the idea and the algorithms of a method for reducing the resonant vibration of the cables in a footbridge. The method relies on change of the static tension in chosen cables of the footbridge. The changes in static tension are introduced when resonance vibration occurs. The paper delineates empirical research employed to experimentally verify the numerical prediction. It has been demonstrated that it is possible to select some stay cables in which applicable change in static tension force value ensures amplitude reduction of forced resonance oscillations of any cable of the whole system. The choice of cables and the magnitude of tension change in them were based on the sensitivity analysis of an eigenproblem formulated in accordance with second order theory. The experimental research was designed to demonstrate practical effectiveness of amplitude reduction of stay cable resonant vibration method. A physical laboratory model of the footbridge was built in compliance with dimensional analysis on a scale of 1:10. Operational Modal Analysis (OMA) method was applied to identifying modal characteristic of a footbridge model.

© 2015 Politechnika Wrocławska. Published by Elsevier Sp. z o.o. All rights reserved.

1. Introduction

Cable-stayed structures, especially bridges and footbridges, have comparatively little stiffness, and are therefore very sensitive to vibration. As the supporting cables are usually the most supple elements of the cable-supported structure, restricting the excessive resonant forced vibration in the cables is often important. The great amplitudes of the transversal forced vibration of the cables are due to small damping and the high suppleness of these elements. The small damping is due to the fact that the cables are usually made of materials with small damping, e.g. steel. Usually, the cables are numerous and of various length. This makes it highly probable that the excitation frequency will become resonance synchronized with one of the many natural frequencies connected to the transversal eigenforms of the cables.

The vibration of the cables may be divided into two groups. The first encompasses the resonant vibration of cables caused by excitations directly acting on the length of the cable, e.g. wind, rain, etc. The second group encompasses resonant vibration of cables caused indirectly by vibration of the deck or pylon, which cause the cable anchor points to oscillate and, as a consequence, lead to kinematic forced vibration of the cables. In most cases, the cause of vibration cannot be eliminated as they are connected to the loads inherent in the

* *Corresponding author*. Tel.: +48 71 320 48 49.
E-mail address: wojciech.pakos@pwr.edu.pl (W. Pakos).
http://dx.doi.org/10.1016/j.acme.2015.09.001
1644-9665/© 2015 Politechnika Wrocławska. Published by Elsevier Sp. z o.o. All rights reserved.

structure's function (e.g. traffic) or are independent of the designers (e.g. climate). Therefore, it is now becoming the more common approach to address not the causes of vibration, but the results – to limit or reduce the amplitudes of the excessive resonant vibration. Usually, *passive devices* are used to reduce cable vibration [1,2]. They are external devices or structure elements built in or attached to the structure, whose function is to create additional motion resistance and, thanks to heightened friction, disperse or absorb the mechanic energy of vibration [3]. Dampers as passive eliminators are characterized by a constancy of parameters (e.g. viscosity coefficients), which cannot be modified during vibration.

It is now becoming more and more common to use *semi-active devices* in reducing the cable vibration in cable-stayed bridges. Among those, there are: semi-active viscotic dampers, semi-active friction dampers, semi-active dampers that change the structure stiffness, and semi-active magnetorheological dampers [1,2], etc. Elements of control systems of semi active equipment can automatically change the dynamic parameters of the system, such as the resistance movement. Semi-active systems of regulation do not destabilize the structure they are affixed to, as they do not add energy to the system; instead, they disperse the energy of its vibration [3].

In the case of long cables, the passive and semi-active devices affixed near the anchoring are ineffective. In such cases, the cable vibration reduction is achieved through cross tying them with lines or stiffer elements. As this is a simple and cheap method, it is the one most often used in vibration reduction when unforeseen resonant vibration of cables occurs [4]. Additionally, special shields, i.e. profiled shielding pipes with internal parallel or spiral ribbing, are used for preventing cable vibration due to wind-rain loads.

In the last three decades, a small number of papers have been published that analyze, theoretically and experimentally, the methods of *active vibration reduction* in cable-supported bridges. Among those discussed is the method of active reduction of cable vibration, which relies on additional forces or vibration which are automatically generated, in real time, in a given point of the structure [2]. The process of active vibration reduction is performed in real time, with a feedback mechanism. After a change in the forces of active adjustment, another measurement is taken to gauge the system response to the excitation. The analysis is repeated until the planned vibration reduction is achieved [2].

A few authors have discussed the use of active vibration reduction in cable-supported bridges. In their 1979 paper [5], Yang and Giannopoulos were the first to consider the use of active vibration reduction in bridge structure under wind load. Using a simple model of a cantilever with a cable, Warnitchai, Fujino et al. [6] showed, both experimentally and analytically, that the vibration connected to the first bending eigenforms of the deck can be reduced using changes in the vibration amplitudes of the cable's anchor point to the deck. Fujino and Susumpow considered the vertical vibration of the cable in the plane of its sag due to the horizontal motion of the foundation and found the method to be effective even for a cable with a small sag [7]. Fujino et al. performed a numerical and experimental analysis of a system consisting of one cable connected to a structure which was a mass with a single degree of freedom. The paper focused on the horizontal cable vibration transverse to the plane of its sag [8].

The algorithms of active vibration reduction presented in the above papers pertain to vibration connected to eigenforms of both the deck and the cables. Achkire [9] presents the analytical and experimental analysis of the method as applied to a single cable and a whole cable structure using Integral Force Feedback (IFF). The motion is performed according to the changing cable tension measured in that anchoring point. Achkire and his co-authors (Preumont, Bossens) give detailed information on the IFF method [10]. In [9], Achkire studied the possible use of flatter vibration reduction in a cable-stayed bridge model in the form of a beam with two cables. The problems of active vibration reduction in civil engineering, including the cable-stayed bridge, are discussed in a comprehensive report of the studies performed between 1997 and 2000 by a number of universities and companies [11].

It must be highlighted that the suggested solutions described above have not yet been implemented in real bridge structures. However, the large number of analytical solutions and experimental studies presented by various authors implies that the application of active methods for reducing vibration in real cable supported bridges will not be long in coming.

2. Aim of the paper

The paper presents the method of resonant stay cable vibration reduction in footbridges and cable-stayed bridges. The method relies on an obvious assumption that it is possible to reduce excessive resonant vibration of any stay cable of a footbridge by change of the static tension in some, purposely selected stay cables [12–14].

The tension tuning method presented in this paper consists in the following. When large resonance vibration occurs in a given cable, a change should be introduced in the static tension of appropriate cables of the system. Usually, the most effective approach is changing the tension in the cable that undergoes the large resonance vibration. However, such a change is not always applicable or even possible. It should also be taken into account that changing the tension of one cable changes the tensions of all the cables in the system. A sensitivity analysis of the eigenproblem of the system makes it possible to determine those cables, in which a tension change will ensure the most effective resonant vibration reduction. It also determines whether the tension should be decreased or increased and what magnitude of the tension change affords the greatest effectivity. The method is made more complex by the fact that the eigenproblem must be formulated according to second order theory. The design parameters in the sensitivity analysis are the tension values in the cables. When the cause of resonant vibration ceases, tensions in the cables return to their initial state.

In the paper, a physical laboratory model of the footbridge, built on a scale of 1:10 is described. Dimensional analysis is also presented in order to explicitly determine the dependence of the magnitude of the elements tested on the model from those occurring in the hypothetical prototype of a footbridge. Some parts of the research were designed to verify compliance

of both: numerical model and laboratory physical model and to validate and attune the FEM numerical model constructed in Cosmos/M environment. Experimental research was also carried out with the use of the model and 34 measure channels system. 32 mini accelerometers and Laser Doppler Vibrometer were used. The laser enabled non-contact stay cable vibration measurements. OMA method does not require intentional vibration excitation of an object. The object might be excited using natural operating conditions or some other excitations might be applied to the object (natural air movement) [15–17].

The main aim of the paper is the final comparison of the results generated by experimental studies with the results of the numerical analyses of the FEM model and to unarguably demonstrate the effectiveness of resonant stay cable vibration reduction in typical footbridges.

3. Laboratory model of a cable-stayed footbridge – dimensional analysis

A physical laboratory model of the steel cable-stayed footbridge, built on a scale of 1:10, was constructed in order to carry out laboratory tests. The laboratory model was created with the utmost conformity to a hypothetical prototype of a real footbridge both in static and dynamic values. Parameters of the model were chosen in a way that would correspond with real steel, short-span cable-stayed bridges, i.e. to be similar to the parameters of a typical footbridge. The main properties of the model to be recreated were: the geometry (length of the span, height of the pylon, slenderness of the deck, etc.), the stiffness of the span (displacement comparison), tension in the stay cables and supporting cables; and eigenfrequencies. The model was designed in such a way that would allow later modifications, such as change of the static system, the number and arrangement of the stay cables, replacing one deck with another, etc. Therefore, when taking into account dimensional analysis, not only parameters of one particular model were considered but also the whole range of parameters that could be applied to all footbridges. Analysis carried out in this way enables future model modifications while retaining dimensional analysis parameters, i.e. enables to try to keep similarity between the model and the prototype [12,14]. This way both work station and the model acquire universal features which consequently might promote further development and generalization of the results presented in this paper and contribute further scientific work of disciplines different than those analyzed in this paper.

Table 1 – Dimensional matrix.

	L_{tot}	L	h_{pyl}	h_p	b	R	σ	δ	E	ν
L_i	1	1	1	1	1	−2	−2	1	−2	0
F	0	0	0	0	0	1	1	0	1	0

Dimensional analysis is the analysis of the relationships between different physical quantities of a prototype (real object) and a model built on a different scale (usually smaller). Dimensional analysis is based on the knowledge of physical quantities which are relevant to the course of analyzed phenomena. A physical quantity is a physical property, such as: force, acceleration, time, frequency of vibration, etc. When choosing physical quantities known and relevant to the analyzed phenomena, one should determine their dimensionless coefficients (products) and check if they will be the same for both the prototype and the model. Based on the similarity of their coefficients one can ultimately determine if the two constructions, built on two different scales will act similarly [18].

The choice of physical quantities is arbitrary to a large extent and also depends on the analyzed physical phenomena [18]. Dimensional analysis in the following research uses the smallest number of physical quantities which thoroughly and accurately characterize the analyzed physical phenomena, such as forced resonance vibrations in footbridges.

When searching for the law of similarity and analysing the static model operation, the following paper employed so called dimensional matrix [18,19] in FLT system (Table 1) where F represents force and L – length.

Geometric parameters were adopted in accordance with Fig. 1: L_{tot} – total theoretical length of the bridge load bearing structure [m]; L – length of the main span [m]; L_1 – length of the side span [m]; h_{pyl} – height of a pylon from the plane of span supports [m]; h – height of a pylon from the base to the plane of span supports [m], h_p – greatest height of the deck's girder [m]; H_p – total height of the pylon [m]; b – width of the deck [m]. The remaining symbols in Table 1 are: R – ultimate tensile cable strength [MPa]; σ – tension [MPa]; δ – displacement [m]; E – Young's modulus [MPa], ν – Poisson's ratio [–].

In dimensional matrix column (Table 1) relevant physical quantities of the analyzed phenomena are presented whereas

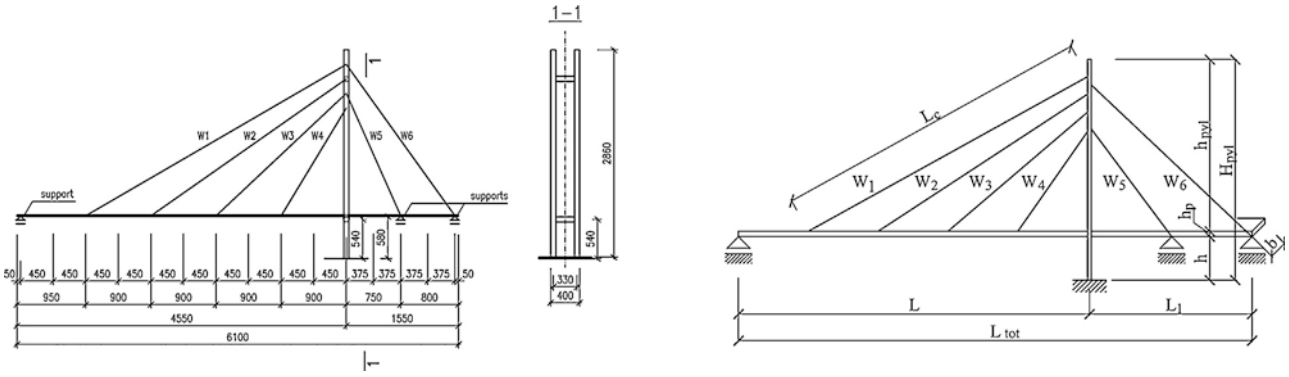

Fig. 1 – Geometry of the footbridge model.

dimensional matrix rows present two basic quantities needed to assess relevant physical quantity. The first quantity is the length (L_i) which could represent the height of a pylon or length of a span. The second quantity is the force (F). Digits that appear in dimensional matrix are the exponents of basic units of measurement that appear in the dimension of the relevant physical quantity. Dimensionless quantities (products) can be based on Table 1. Dimensionless quantities (m) (product) were created in accordance with Buckingham π theorem, also known as pi-theorem, which is a key theorem in dimensional analysis. The number of products (m) is equal to the number of physical parameters introduced (s) that are reduced by the number of basic parameters (r) [18,20]. The number of dimensionless quantities (products) equals $m = s - r = 10 - 2 = 8$. The following set of dimensionless coefficients (products) is called a complete set of dimensionless coefficients when each of them is independent from the others [18,19]. In other words, two constructions which have been described by means of these 10 physical quantities act identically regardless of their size and loads provided that 8 dimensionless ratios are the same both in the prototype and the model [18]. It is also possible to use the dimensional analysis proposed in this research for a cable-stayed construction where geometric nonlinear dependencies occur [18].

It should be pointed out that ratio of all the physical quantities of the model and the prototype might take different scales. While testing the cable-stayed footbridge model, a scale based upon a length ratio expressed in the form of a quotient was adopted:

$$L_V = \frac{L_M}{L_P} \tag{1}$$

where L_M – length used in the model, L_P – length used in the prototype. Scale of L_V equals 1:10. Table 2 shows relevant geometrical and material properties of the model based on this scale.

All other dimensionless quantities were determined.

- *Proportions of span's length*. One-pylon bridges: $L = (0.6 - 0.7)\, L_{tot}$ [1]

$$\frac{L_M}{L_{tot,M}} = \frac{L_P}{L_{tot,P}}; \quad \frac{4.5}{6.0} = \frac{45}{60}; \quad 0.75 = 0.75 \tag{2}$$

- *Pylon height*. Theoretical ratio of pylon height above the deck to the main span (h_{pyl}/L) for one-pylon bridge:
  - Radial cable system (fan like cable arrangement): $h_{pyl,M}/L = 0.4$,
  - Harp cable system requires slightly higher pylons: $h_{pyl,M}/L = 0.5$ [1].

  The height of the pylon should not exceed 20–25 m [1]. When using static scheme, Fig. 1:

$$\frac{h_{pyl,M}}{L_M} = \frac{h_{pyl,M}}{L_P}; \quad \frac{2.285}{4.5} = \frac{22.85}{45}; \quad 0.51 = 0.51 \tag{3}$$

- *Width of the deck*. Decks of the footbridges are usually narrow, from 2 to 5 m, rarely above 7 m [1]. When using static scheme, Fig. 1:

$$\frac{b_M}{L_M} = \frac{b_P}{L_P}; \quad \frac{0.25}{4.5} = \frac{2.5}{45}; \quad 0.06 = 0.06 \tag{4}$$

- *Height of the main girder*. When using two rows of cables which are arranged densely $h_p/L = 1/285–1/150$ [1]. When using static scheme, Fig. 1:

$$\frac{h_{p,M}}{L_M} = \frac{h_{p,P}}{L_P}; \quad \frac{0.015}{4.5} = \frac{0.15}{45}; \quad 0.0033 = 0.0033. \tag{5}$$

  However, more important appears to be the girder rigidity similarity condition, that is, a comparison between the model and the prototype displacement.

- *Deck displacement*. On the basis of numerical analysis, maximum displacement of the main span was obtained $\delta_M = 0.0126$ m so assuming appropriate span length of the prototype it is possible to determine δ_P displacement of the prototype's main span. When using static scheme Fig. 1: $(6) \frac{\delta_M}{L_M} = \frac{\delta_P}{L_P}; \quad \frac{0.0126}{4.5} = \frac{\delta_P}{45}; \quad \delta_P = 0.126\,\text{m}$.

  In the prototype $\delta_P = 0.126$ m displacement is an obtainable quantity and falls within the actual construction parameters. Displacement of both constructions is geometrically similar.

- *Equality condition of Poisson's ratio ν and Young's modulus E*.

  Poisson's ratio ν is a natural and practically unchangeable material constant. Satisfying coefficients equality condition of Poisson's ratio and Young's modulus, is this case, is not difficult since steel was used as the construction material in both the prototype and the model.

$$\nu_M = \nu_P; \quad E_M = E_P \tag{7}$$

- *Stress in stay cables*. Under operational load, acceptable cable stress of bridge constructions should not exceed 0.3–0.45 of ultimate tensile cable strength R_{pk} [1]. The cables effort in different characteristic load conditions of the model were presented in the paper [12]. Assumed characteristic strength of cables $R_{pk} = 1770$ MPa.

Dimensional analysis can also be applied to issues of dynamics [18,19]. However, when describing dynamic phenomena, it is better to apply so called mass system which is characterized by three main basic quantities: mass (M), length (L) and time (T) [18,19]. When determining model similarity

Table 2 – Geometrical and material quantities of the model (M) and the prototype (P).

	Symbol									
	L_{tot} [m]	L [m]	L_1 [m]	h_{pyl} [m]	h [m]	H_{pyl} [m]	h_p [m]	b [m]	E [GPa]	ν [–]
Geometric parameters of the model	6.0	4.5	1.5	2.285	0.58	2.88	0.015	0.25	205	0.3
Geometric parameters of the prototype	60.0	45.0	15.0	22.48	5.80	28.8	0.15	2.5	205	0.3

regarding dynamic features of the model and the prototype, e.g. when determining eigenfrequencies of the object, it is essential to select appropriate mass and stiffness of the spans. Dynamic similarity was determined on the basis of the formula (9) [21]:

$$\frac{\omega_{i,M}}{\omega_{i,P}} = \sqrt{\frac{m^o_{i,P} \cdot k^o_{i,M}}{m^o_{i,M} \cdot k^o_{i,P}}}. \tag{8}$$

where $\omega_{i,M}$, $\omega_{i,P}$ – total eigenfrequency of the model and the prototype respectively; $m^o_{i,M}$, $m^o_{i,P}$ – total generalized mass of the model and the prototype respectively corresponding to the total frequency; to the total frequency; $k^o_{i,M}$, $k^o_{i,P}$ – total generalized stiffness of the model and the prototype respectively corresponding to the total frequency.

By means of FEM numerical model (Cosmos/M) it was possible to determine total eigenfrequencies of the model and the main mass and stiffness corresponding to these frequencies. Then, by using dimensions of the construction elements and material parameters obtained with dimensional analysis, a numerical model of the prototype was constructed on the basis of which the main stiffness and mass were obtained. For instance, obtained eigenfrequency corresponding to the vertical eigenform of the deck is 1.55 Hz and remains within such range of eigenfrequencies that can be observed in real cable-stayed footbridges [22]. This indicates model similarity to the prototype.

Fig. 2 – The model of the footbridge in laboratory, the Institute of Civil Engineering.

4. Geometrical and material parameters of the laboratory model and initial cable tension force

A steel, cable-stayed model of the footbridge was designed and created with a total length L_{tot} = 6.0 m and a pylon height H_{pyl} = 2.86 m (see Fig. 2). The model of the footbridge was made entirely of steel. The model consists of both welded and screw-fastened elements that allow assembling and disassembling of the elements. Fig. 1 presents the basic geometrical traits of the real physical model of the cable-stayed footbridge with the assumed parameters and symbols. The symbols in Tables 1 and 2 correspond to the ones in Fig. 1.

Fig. 3 presents construction details and cable tension regulators which are fixed to all stay cables. These regulators enable to easily shorten or lengthen the cables within ±30 mm. The cables were made of type 1 × 19 lines, d = 1.2 mm; d = 1.8 mm dia., and tensile strength f_y = 1770 MPa.

Stay cable forces were chosen in such a way as to settle the deck's grade line at a level of ±0.00 m. The choice of initial tension forces was based on numerical analysis.

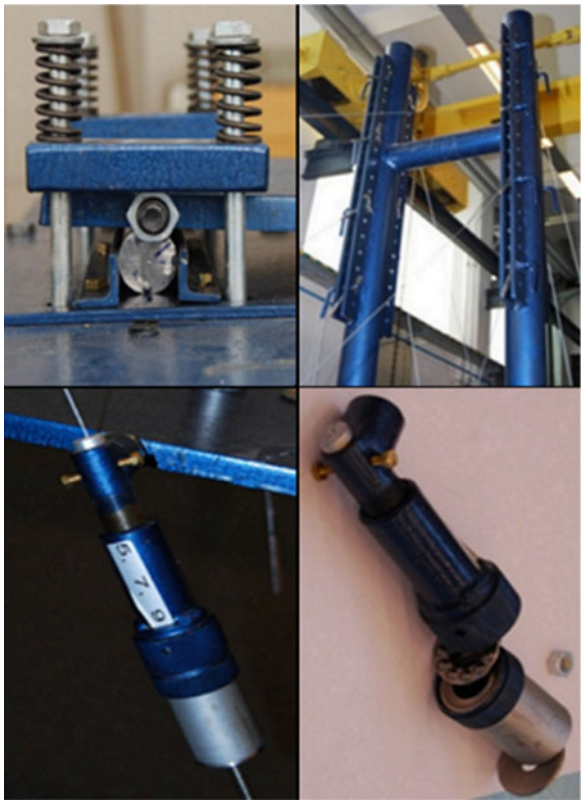

Fig. 3 – Tension regulator and construction details.

5. Frequencies and eigenforms of the laboratory footbridge model

Fig. 4 presents OMA measuring pattern which was used to depict eigenforms obtained. Fig. 4 also presents distribution of measurement points. Accelerometers and the direction of acceleration measurement, which were fixed on the measurement points, were marked with green arrows. Fig. 5 presents

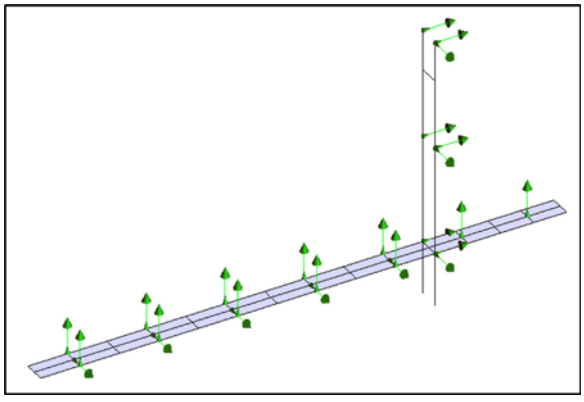

Fig. 4 – Measurement points and the direction of acceleration measurement with OMA.

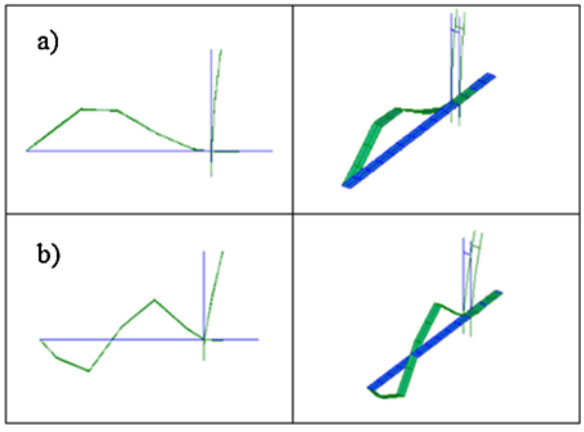

Fig. 5 – The first (a) and second (b) eigenform corresponding to eigenfrequency f_1 = 5.66 Hz and f_1 = 11.48 Hz obtained with OMA.

exemplary eigenforms which were identified with OMA algorithms.

Table 3 compares footbridge eigenfrequencies experimentally determined with OMA with the use of physical laboratory model and eigenfrequencies numerically calculated with the use of validated and adjusted numerical FEM model constructed in Cosmos/M environment. The last column presents approximation error magnitude of both ways of eigenfrequency determination.

Stay cables eigenfrequencies were measured and later compared to eigenfrequencies obtained with numerical model in Cosmos/M and to eigenfrequencies obtained from analytical solutions based on Irvine's formula (cf. Table 4). Commonly known Irvine's formulas $f_{I.wp}$, $f_{I.zp}$, represent eigenfrequencies of a cable which is isolated from the whole construction, respectively eigenfrequencies for the eigenform in the plane of the sag (*wp*) and eigenfrequencies for the eigenform out-of-plane of the sag (*zp*). Parameter λ^2 is Irvine's parameter. The non-contact measurements were conducted via Doppler laser. Numerals on the cables are presented in Fig. 1.

6. Influence of tension change on eigenfrequencies of the physical model

The following section of the paper concentrates on some results of the experimental research and analyses the influence of tension change of individual six pairs of stay cables on change of eigenfrequencies of the physical model of the footbridge. As an example, graphs in Fig. 6a and b presents frequencies values (red color) measured on the physical model with the force change in the 2nd and 3rd pair of stay cables respectively. Green color indicates changes of frequencies values of a stay cable which was subject to force changes. The graphs in Fig. 6c indicated in green show changes in the frequency corresponding to the eigenforms with dominant transversal motion (vibration) in all cables with the force change in the 2nd pair of stay cables. Vertical line on the graph represents individual cables tension in the initial state and eigenfrequencies corresponding to these tensions. Initial state means that the forces in the cables are selected in such a way as to settle the deck's grade line under a loading condition, involving only its own weight, at a level of ±0.00 m. The analyses were carried out within a wide range of design parameters variability, ranging from 0% to 20% of their maximal, acceptable characteristic load-carrying capacity, marked with N_k.

Based on the results of the tests on the influence of tension change of individual pairs of stay cables on change of eigenfrequencies related to eigenforms of the deck and the pylon, it can be noted that:

- there is very high consistency between modal analysis results carried through OMA algorithms based on experimental

Table 3 – Model frequencies experimentally measured (OMA) and calculated in Cosmos/M.

Form number	Form description	*f* [Hz]		The relative error
		OMA	Cosmos/M	
1	Deck – 1st bending form	5.66	5.60	1.0%
2	Deck – 2nd bending form	11.54	11.48	0.5%
3	Pylon – 1st plane bending form	15.48	14.77	4.8%
4	Deck – 3rd bending form	19.94	20.10	−0.8%
5	Deck – 4th bending form	31.18	32.16	−3.1%
6	Deck – out-of-plane form	35.12	37.16	−5.5%
7	Deck – torsional form	36.96	44.59	−17.1%
8	Deck – 5th bending form	47.21	47.45	−0.5%

Table 4 – Eigenfrequencies of stay cables.

Design. cable	$f_{e.P}$ [Hz]	$f_{e.L}$ [Hz]	$f_{l.wp}$ [Hz]	$f_{l.zp}$ [Hz]	$f_{c.wp}$ [Hz]	$f_{c.zp}$ [Hz]	η_1 [%]	η_2 [%]	η_3 [%]	η_4 [%]
W_1	23.38	23.38	23.2091	23.2085	23.4096	23.4014	0.74%	0.74%	−0.13%	−0.13%
W_2	26.75	26.38	26.5422	26.5414	26.7635	26.7626	0.78%	−0.61%	−0.05%	−1.43%
W_3	35.38	35.25	35.3168	35.3163	35.6232	35.6167	0.18%	−0.19%	−0.68%	−1.05%
W_4	40.37	39.50	42.5126	42.5118	42.9146	42.9131	−5.04%	−7.09%	−5.93%	−7.96%
W_5	46.13	45.00	47.4242	47.4240	47.4599	47.4551	−2.73%	−5.11%	−2.80%	−5.18%
W_6	29.38	29.00	30.5938	30.5932	30.6166	30.6106	−3.97%	−5.21%	−4.04%	−5.28%

$f_{e.L}$, $f_{e.P}$ – obtained experimentally; L – left cable, P – right cable.
$f_{c.wp}$, $f_{c.zp}$ – eigenfrequencies obtained with numerical model in Cosmos/M.
$\eta_1 = f_{e.p}/f_{l.wp}$; $\eta_2 = f_{e.L}/f_{l.wp}$; $\eta_3 = f_{e.P}/f_{c.wp}$; $\eta_c = f_{e.p}/f_{c.wp}$.
Irvin formula: $f_{l.zp} = \omega_n/2\pi = n/2L \cdot \sqrt{N/m}, \quad n = 1, 2, 3, \ldots$.

$f_{l.wp} = \omega_n/(2\pi) = \mathring{\omega}_n/2\pi L \cdot \sqrt{N/m}, \quad n = 1, 2, 3, \ldots; \quad \tan(\mathring{\omega}_n/2) = \mathring{\omega}_n/2 - 4/\lambda^2 \cdot (\mathring{\omega}_n/2)^3$.

measurements carried out on a physical laboratory model and results obtained from calculations based on Cosmos/M FEM numerical model;
- there is a very limited influence of cable tension change on eigenfrequencies changes corresponding to eigenforms of the pylon and the deck;
- there is consistency between results obtained with numerical method and the experimental research results related to the influence of actual disconnection of one pair of cables on eigenfrequencies of the model.

The results achieved demonstrate the validity of the theory applied in numerical modeling and accordance between the physical and numerical model of the footbridge.

7. Eigenproblem sensitivity analysis

Sensitivity analysis of the eigenproblem of the system was used in order to determine the influence of tension change in one cable – or a few cables – on the change of eigenfrequencies of the footbridge. This procedure makes it possible to determine theoretically what tension change, and in which cable, will cause the greatest change in the chosen eigenfrequency of the system, and especially of the chosen cable. From a mathematical point of view, the sensitivity analysis of the eigenproblem is a calculation of the derivative of the matrix solution of a homogenous differential equation of motion of the system, with respect to a given design parameter p. In this case, the design parameter p is the tension force in cable N. Theoretical value of the logarithmic sensitivity function was calculated in the paper [12]. In the paper [12] the effectiveness of the method was tested using FEM model of a footbridge, on the basis of algorithms developed in Cosmos/M and *Mathematica*.

Table 5 presents values of the logarithmic sensitivity function calculated on the basis of both experimentally calculated eigenfrequencies of the physical model and measurements of tension on stay cables. Calculations were performed using simplified formula (incremental)

$$s_i = \frac{\Delta\omega_i/\omega_i}{\Delta N_i/N_i} \tag{9}$$

which specifies approximate coefficients of logarithmic sensitivity function. Due to the change of cables tension, only values of the logarithmic sensitivity function referring to eigenfrequencies of stay cables were determined. Logarithmic sensitivity function referring to eigenfrequencies related to

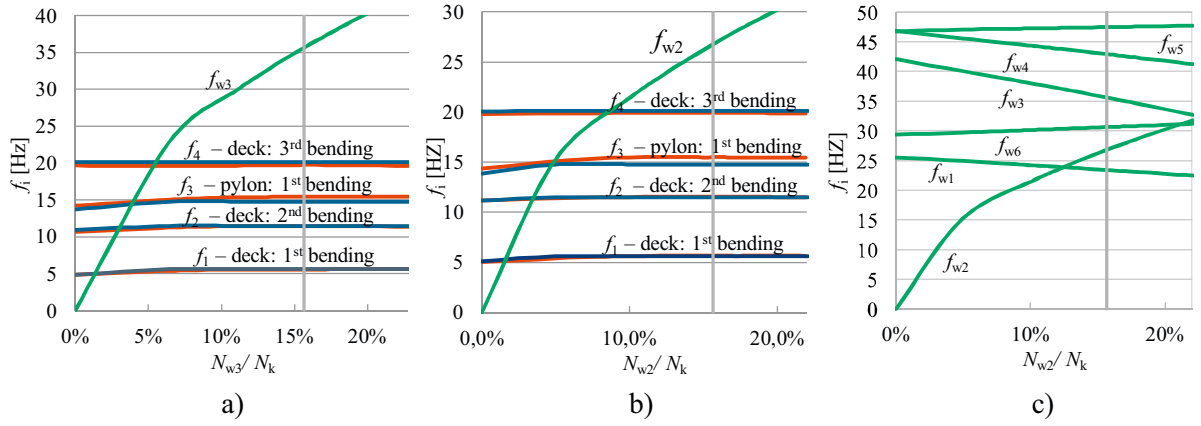

Fig. 6 – Influence of W_3 cables (a) and W_2 cables (b and c) effort change on the change of eigenfrequencies of the physical and numerical model; eigenfrequencies: experimentally measured; obtained with Cosmos/M corresponding to eigenforms: of the deck and the pylon, stay cables.

Table 5 – Experimental values of the logarithmic sensitivity function s_i acknowledging cable tension changes on cable pairs.

	Cable numer – eigenforms	N_1	N_2	N_3	N_4	N_5	N_6
ω_{1w}	Cables no. 1 – in plane	**0.48166**	–0.05811	–0.06779	–0.01583	0.08964	0.11361
ω_{2w}	Cables no. 2 – in plane	–0.25184	**0.48400**	–0.18960	–0.03912	0.04166	0.05280
ω_{3w}	Cables no. 3 – in plane	–0.10893	–0.16252	**0.53575**	–0.11794	0.00696	0.00883
ω_{4w}	Cables no. 4 – in plane	–0.04175	–0.02412	–0.31488	**0.51445**	0.01877	0.02378
ω_{5w}	Cables no. 5 – in plane	0.05095	0.03223	0.00628	0.00588	**0.47985**	–0.11271
ω_{6w}	Cables no. 6 – in plane	0.09848	0.04581	0.02676	0.01672	–0.16373	**0.48384**

eigenforms of the deck and the pylon were not determined since eigenfrequency changes were too low to experimentally and reliably determine values of the logarithmic sensitivity function. Columns marked with N_i in Table 5 present cable tension changes affecting changes of individual eigenfrequencies (i – number of stay cable pairs), e.g. column N_1 indicates how tension change in stay cable pair number one influenced eigenfrequency change of individual cables marked from ω_{1w} to ω_{6w}.

Table 5 presents values of the logarithmic sensitivity function calculated on the basis of experimentally determined eigenfrequencies of the physical laboratory model. In the paper [12] shows values of the logarithmic sensitivity function theoretically calculated with the use of FEM numerical model. On the basis of comparison of both analyses (numerical and experimental) we can see that they are comparable with regard to absolute value and they have the same symbols.

8. Stay cable vibration reduction – examples

Measurement exciter and power amplifier were used for resonant vibration excitation of the physical model. The exciter was connected to the deck by a stiff cable and the structure was excited by a harmonic force. The exciter was attached to the longer bridge span, 2.0 m away from side deck support (Fig. 7). Harmonic force used ranged from 10 N to 20 N with frequency equal to eigenfrequency of one, selected stay cable.

For the purposes of a numerical solution of the FEM footbridge model, in which damping is taken into account, the parameters of three damping models were determined. The following models were analyzed: mass, Voigt–Kelvin and Rayleigh. The description of damping model variants and the way their coefficients were chosen was presented in detail in the unpublished paper [12]. This paper only presents a comparison between the results of experimental studies of a footbridge model with an attached, but non-functioning vibration exciter, and the results of numerical analyses of this model tuned in such a way that it takes into account the attached exciter, and thus the possible damping that could occur during resonant vibration excited by the exciter. A numerical analysis of three damping models was performed [23]:

- mass (mass-proportional damping, $\mathbf{C} = \alpha \cdot \mathbf{B}$),

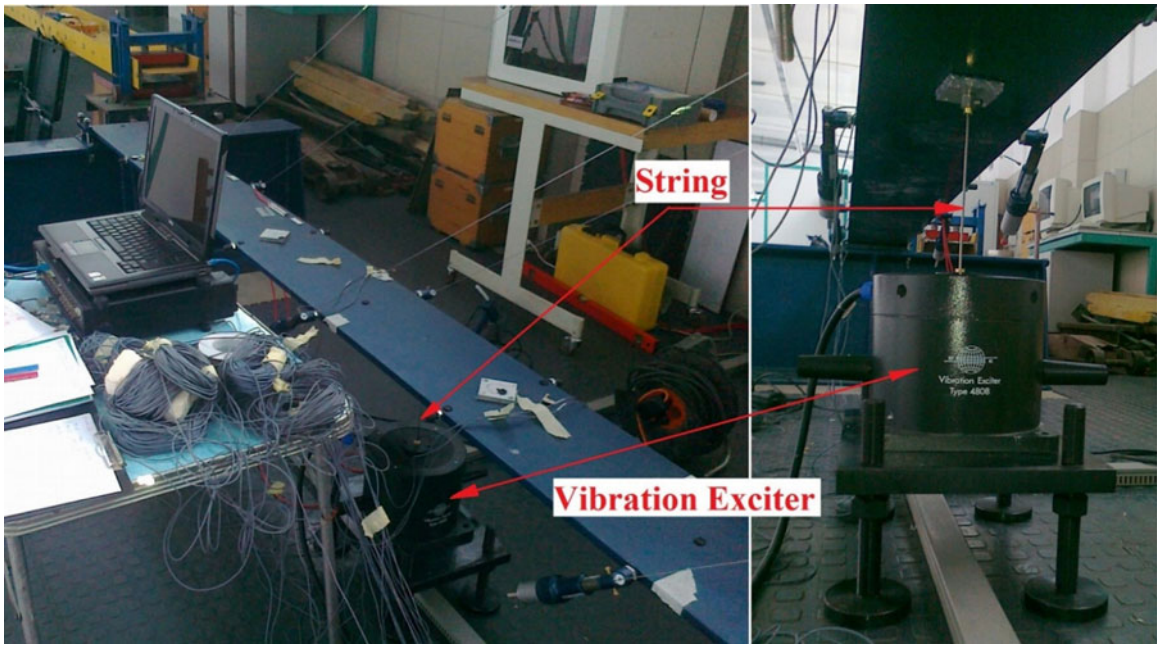

Fig. 7 – Vibration exciter.

- Voigt–Kelvin (stiffness-proportional damping, $\mathbf{C} = \beta \cdot \mathbf{K}$)
- Rayleigh (both mass- and stiffness-proportional damping, $\mathbf{C} = \alpha \cdot \mathbf{B} + \beta \cdot \mathbf{K}$).

First, the logarithmic decrement of the damping was determined using an experimental method in the process of free vibration. The formula $\delta = \ln q(t)/[nq(t + nT')]$ was used, where it was assumed that $n = 100$. Then, the value of the non-dimensional damping ratio was found from $\xi = \delta/\sqrt{4\pi^2 + \delta^2} = 0.002015$. Following this, the values of the damping parameters were determined: α – dimensional mass-proportional damping coefficient (in inverse of second) and β – dimensional stiffness-proportional damping coefficient (retardation time in seconds), which were then used to create corresponding damping matrix models for the three considered damping models. The following values were found:

- value of parameter α of the mass damping model, corresponding to the first bending eigenform of the deck with an eigenfrequency of $f_1 = 5.601$ Hz, which is then $\alpha = \gamma \cdot \omega_i = \gamma 2\pi f_1 = 0.142\ \mathrm{s}^{-1}$, where $\gamma = 2\xi = 0.00403$;
- value of parameter β of the Voigt–Kelvin model for the same frequency $f_1 = 5.601$ Hz, which is then $\beta = \gamma/\omega_1 = \gamma/2\pi f_1 = 0.000115$ s;
- values of parameters α and β in the case of the Rayleigh model, where a set of two equations was solved, $\gamma_i = \alpha/\omega_i + \beta\omega_i$ and $\gamma_j = \alpha/\omega_j + \beta\omega_j$, in which it was assumed that the coefficients $\gamma_1 = \gamma_2 = \gamma = 0.00403$ are equal for two chosen eigenfrequencies, i.e. eigenfrequency $f_1 = 5.601$ Hz, connected to the first bending eigenform of the deck, and eigenfrequency $f_2 = 11.477$ Hz connected to the second bending eigenfrequency of the deck – the following parameters were obtained: $\alpha = 0.095311\ \mathrm{s}^{-1}$ and $\beta = 0.0000376$ s.

In order to choose the appropriate variant of the damping model, fragments of time histories of the velocity of chosen points of the structure were compared. In the laboratory model, the exciter functioned with an eigenfrequency $f_1 = 5.601$ Hz, connected to the first bending eigenform of the deck. A comparison between the time histories of the velocity of damped resonant vibration of the cable W_{1P} is shown in Fig. 8. Fig. 8a shows the vibration process identified experimentally in the laboratory model. Fig. 8b–d shows the time histories of the vibration velocities for the three damping models described above, determined numerically using the system Cosmos/M. The damping parameters for those three models were determined experimentally in a process of free vibration of the model of the structure with an attached, but non-functioning exciter.

On the basis of a comparison between the results of the experimental studies (Fig. 8a) and the results of numerical analyses (Fig. 8b–d), it can be found that the Rayleigh model (Fig. 8b) with parameters $\alpha = 0.095311\ \mathrm{s}^{-1}$ and $\beta = 0.0000376$ s is the only one that describes vibration damping in the footbridge model appropriately. It is only for the Rayleigh model that the determined amplitudes of resonant vibration reach values close to the experimentally determined ones. Therefore, the Rayleigh model was used in further numerical analyses in order to compare the results of theoretical and experimental studies.

Furthermore, a comparison of the graphs in Fig. 8 reveals that assuming the mass damping model leads, in this case, to needlessly heightened values of the vibration velocity

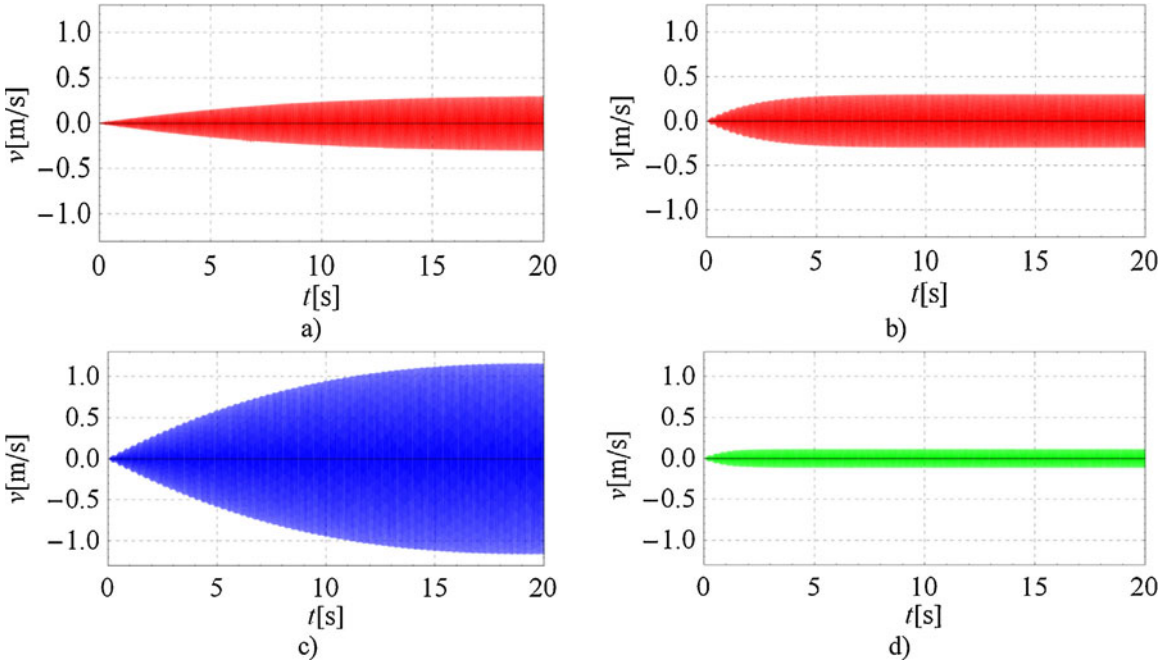

Fig. 8 – Velocity amplitudes of cable mid-span W_{1P} under resonant harmonic excitation: (a) measured, (b) Rayleigh's damping model: $\mathbf{C} = \alpha \cdot \mathbf{B} + \beta \cdot \mathbf{K}$, $\alpha = 0.095311\ \mathrm{s}^{-1}$ and $\beta = 0.0000376$ s, (c) mass damping model $\mathbf{C} = \alpha \cdot \mathbf{B}$, $\alpha = 0.142\ \mathrm{s}^{-1}$, (d) Voigt–Kelvin damping model $\mathbf{C} = \beta \cdot \mathbf{K}$, $\beta = 0.000115$ s.

amplitudes (see Fig. 8a and c). This may be due to the fact that the mass model is connected only to the external, environment based resistance to motion. The Voigt–Kelvin model, on the other hand, yields lowered results of the amplitudes (see Fig. 8a and d), probably due to the fact that it assumes that the resistance to motion is of an internal nature (due to the material of the structure). In reality, damping is caused by both these factors; the Rayleigh model takes this into account and thus leads to the best concordance between the theoretical and experimental results.

In this paper, a structure is analyzed to which an exciter was attached throughout the experiment (Fig. 7). Initially, in the process of free vibration, the exciter was not functioning at all. In the second phase of the experiment, the exciter was functioning and resulted in the occurrence of resonant vibration in the cables of the footbridge. Both during free vibration and during resonant vibration, the whole system of model-exciter was analyzed (Fig. 7). Even should damping during resonant vibration have a slightly different value than during free vibration, this fact would have no bearing on the main aim of this paper, which was to present the significant influence of changing the tension in cables on the reduction of resonant vibration in the cables of a footbridge model. It should also be highlighted that the numerical model was tuned in such a way that it took into account the attached exciter, and thus its possible damping effect on the model structure. This may be attested to, indirectly, by the close convergence of the theoretical predicted and experimentally verified results.

Firstly, stay cable W_{1P} vibration reduction was analyzed. This cable was harmonically excited with 20 N force with frequency that equaled to eigenfrequency of the stay cable, i.e. approx. $f_{w1P} = 23.5$ Hz. Vibration reduction was accomplished by a force change in W_{6P} cable, from the initial effort 16.2% to 54.5%. Effort is identified here as force ratio (in %) of a cable under a certain loading condition to permissible characteristic load-carrying capacity of this cable. Change of pulling force (tension) started in 40th second of resonant vibration excitation. After subsequent 5 s, the effort achieved was equal to 54.5%. The result of vibration reduction is presented in blue in Fig. 9. Red color was used to mark fixed resonant state, i.e. such damping resonant oscillations which occurred when cable tension was not changed. As it can be seen (cf. Fig. 9) significant change (up to 96%) of tension in cable number 6 largely reduces amplitudes of forced resonance oscillations in cable one.

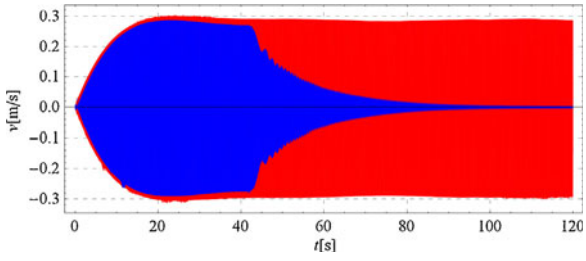

Fig. 9 – Influence of W_{6P} cable tension change on velocity amplitudes change of resonant transverse vibration of W_{1P} cable; without W_{6P} cable tension change; the result of W_{6P} cable tension change.

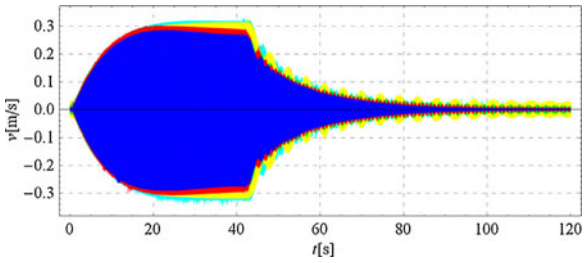

Fig. 10 – Influence of different W_{6P} cable tension changes on velocity amplitude change of the resonant transverse vibrations of W_{1P} cable mid-span.

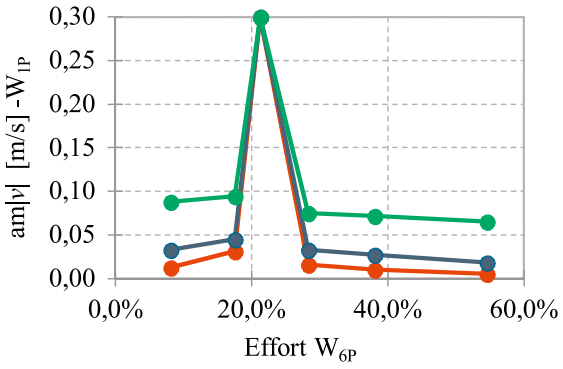

Fig. 11 – Maximum velocity amplitudes of W_{1P} cable with variable effort of W_{6P} cable measured in: 110–115 [s], 80–85 [s], 60–65 [s] of vibration reduction process.

Fig. 10 shows the result of cable W_{1P} tension reduction under different value changes of cable W_{6P} tension. The force change was introduced between 40th to approx. 50th second after vibration excitation started. Blue color shows recorded fragment of timing parameters of W_{1P} cable mid-span velocity under W_{6P} cable effort change ranging from 16.2% to 54.5% of the initial effort state.

Red color shows influence of effort change by approx. 38.0%, green – 28.4%, yellow – 17.6%, azure – 8.1%. Initial state was achieved after each effort change on W_{6P} cable initial state was achieved. It was followed by a series of different effort changes of stay cables which were measured.

Fig. 11 shows the maximum velocity amplitude of the resonant transverse vibration of W_{1P} cable mid-span under few stay cables effort changes. The maximum amplitude was measured after timing parameters were stabilized and vibration reduced, i.e. approx. 110–115th second (red color) and also within vibration stabilizing stage, approx. 80–85th second, (blue color) and about 60–65th second (green color). With a 6.7% force change on W_{6P} cable it was possible to reduce the velocity amplitudes of resonant transverse vibrations of the W_{1P} cable mid-span in the range of 55–65% whereas 17.3% force reduction on W_{6P} cable caused reduction of velocity amplitudes of resonant transverse vibration of the W_{1P} cable mid-span up to 85.7%. Reducing force value in W_{6P} cable by about 60–80% caused reduction of velocity amplitudes of the resonant transverse vibrations of W_{1P} cable mid-span by approximately 96%.

Fig. 12 presents a comparison of the results obtained in Cosmos/M calculations to the results of measurements. It shows the maximum velocity amplitudes of forced transverse vibration of cables W_{1P} as a function of the changes of static tension force in cables W_{6P}. In the numerical analysis, the Rayleigh damping model was assumed.

An important conclusion can be drawn after the experimental results analysis. It indicates that slight tension change of properly selected cable is sufficient to significantly reduce excessive resonant vibrations in a different stay cable. Theoretical and experimental sensitivity analysis carried out revealed that tension change in cable number three can effectively change eigenfrequencies of cables two, three and four (Table 5) and accordingly experimental verification of resonant vibration reduction of selected stay cables was performed.

Fig. 13 presents influence of W_{3P} cable tension change on velocity amplitudes of the forced resonance vibrations of the W_{2P} cable mid-span. The excitation was performed with harmonic force of 17 N with frequency equal to eigenfrequency ($f_{w2P} \approx 26.75$ Hz) of a stay cable. In this case it can also be seen that the influence of W_{3P} cable tension change significantly (up to 97%) reduces amplitudes of forced resonance oscillations of W_{2P} cable (cf. Fig. 13).

Fig. 14 compares the effect of W_2 cable tension reduction obtained by tension change on one cable (W_{3P} cable) to tension reduction performed on cable pairs number three, i.e. W_{3P}, W_{3L}. Nature of vibration disappearance in both cases is similar

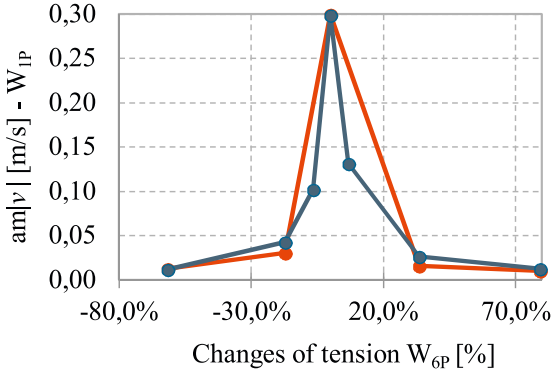

Fig. 12 – The maximum velocity amplitudes of forced transverse vibration of cables W_{1P} as a function of the changes of static tension force in cables W_{6P}; measured, Cosmos/M.

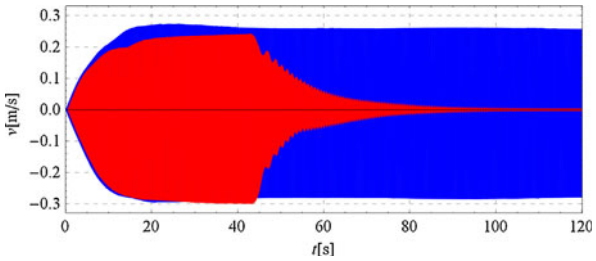

Fig. 13 – Influence of W_{3P} cable effort change on velocity amplitude change of W_{2P} cable initial state (without W_{3P} cable tension change); effect of W_{3P} cable tension change.

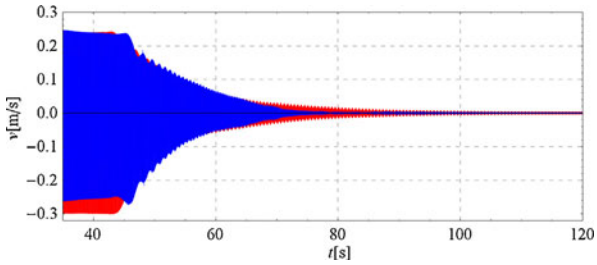

Fig. 14 – Influence of W_{3P} cable effort change ( ) and two cables W_{3P} and W_{3L} ( ) on velocity amplitude change of W_{2P} cable.

and no particular differences in velocity amplitudes over the period of time are visible. The measurements indicate that it is enough to change the tension only in one pair of cables to obtain sufficient vibration reduction effect. It is possible thus to install less cable tension regulators which lowers the costs of a vibration reduction system.

9. Conclusions

The experimental and numerical (FEM) studies have demonstrated that:

- it is possible to significantly change the tension of selected stay cables without causing considerable changes of eigenfrequencies corresponding to eigenforms of a deck and a pylon. It is indicated by low value of logarithmic sensitivity function related to changes of eigenfrequencies;
- tension change of one or of several stay cables can significantly reduce forced resonance vibration of any other stay cable;
- tension change of each of the stay cables always significantly influences the frequency of the cable which was subject to force change;
- it is sufficient to change the tension in one cable of a pair since the nature and rate of vibration disappearance is similar to the one we observe when changing tension in both cables of a pair;
- sensitivity analysis requires application of second order theory to describe eigenproblem of the cable-stayed objects;
- there is no need to take into account the influence of large displacements on eigenproblem of cable-stayed constructions, so it is reasonable to simplify geometrically nonlinear theory (second order theory) in an algorithm of sensitivity analysis of eigenproblem with respect to tension change of stay cables.

10. Summary

The numerical and experimental framework of this paper demonstrates that the method of reduction of forced resonance oscillations of cables in cable-stayed footbridges by the change of the static tension in some stay cables is effective and

is a viable alternative to currently used methods of reduction of forced resonance oscillations. The method of reduction of vibrations comes down to changes of static tension forces in some, selected stay cables. The change of force takes place automatically, in real-time, i.e. when excessive force resonance oscillations of any stay cables occur. Choice of cables, which are subject to static tension changes, is not accidental. It is based on previously performed sensitivity analysis of eigenproblem with respect to the variability of design parameters, i.e. stay cables tensions. In sensitivity analysis the eigenproblem has to be formulated according to the second order theory.

It has been theoretically and experimentally demonstrated that proper combination of tension changes in stay cables ensures significant reduction of not only the excessive force resonance oscillations of the cables, which were the subject of tension changes, but also in other cables.

Effectiveness of the vibration reduction method was tested with resonant forced vibrations. Numerical and experimental research was carried out under harmonic excitations. Harmonic excitations may occur in reality in footbridges in the case of force i.e. caused squats people [24].

Experimental tests and numerical analyses support the validity of the proposed method of reduction of cable vibration in cable-stayed footbridges. Practical effectiveness of the method can be confirmed by the results which indicate that it is sufficient to attach the tension changing device only to some, selected cables in order to significantly reduce resonant vibration in any cable of the whole system. The proposed method can serve as an alternative to current methods of vibration reduction which use vibration dampers and eliminators. The proposed method of cable vibration reduction in stay cables is easier than other methods of active reduction of cable vibration that were presented in scientific works [9,10] which use dynamic tension changes of cables.

The advantages of using the proposed method are particularly applicable to long cables since passive and semi-active vibration eliminators installed in the proximity of an anchor prove ineffective. Moreover, the proposed method of vibration reduction recognizes that there is no need to determine the cause of excessive resonant vibrations. The aim of this method is to counteract resonant vibration by changing eigenfrequency values of the cables and not by changing excitation forces.

The authors hope that this article will significantly broaden the knowledge of vibration reduction of stay-cabled systems. They also believe that the method of vibration reduction by the change of static tension of stay-cables will become a useful engineering device and its implementation will contribute to designing and building safer bridge structures.

REFERENCES

[1] J. Biliszczuk, Cable-Stayed Bridges. Design and Implementation, Arkady, Warszawa, 2005 (in Polish).

[2] E. Caetano, Cable Vibration in Cable-Stayed Bridges, IABSE-AIPC-IVBH ETH Honggerberg, Zurich, Switzerland, 2007.

[3] Z. Osiński, Damping of Vibrations, Wydawnictwo Naukowe PWN, Warszawa, 1997 (in Polish).

[4] H. Yamaguchi, H.D. Nagahawatta, Damping effects of cable cross tie in cable-stayed bridges, Journal of Wind Engineering and Industrial Aerodynamics 54/55 (1995) 35–43.

[5] J. Yang, F. Giannopoulos, Active control and stability of cable-stayed bridge, Journal of the Engineering Mechanics Division 105 (4) (1979) 677–694.

[6] P. Warnitchai, Y. Fujino, B.M. Pacheco, R. Agret, An experimental study on active tendon control of cable-stayed bridges, Earthquake Engineering & Structural Dynamics 22 (1993) 93–111.

[7] Y. Fujino, T. Susumpow, An experimnental study on active control of in-plane cable vibration by axial support motion, Earthquake Engineering and Structural Dynamics 23 (1994) 1283–1297.

[8] Y. Fujino, P. Warnitchai i, B.M. Pacheco, Active stiffness control of cable vibration, Journal of Applied Mechanics 60 (4) (1993) 948–953.

[9] Y. Achkire, Active Tendon Control of Cable Stayed Bridges, (Ph.D. thesis), Active Structures Laboratory, Universite Libre de Bruxelles, Belgium, 1997.

[10] Y. Achkire, F. Bossens, A. Preumont, Active damping and flutter control of cable-stayed bridge, Journal of Wind Engineering and Indystrial Aerodynamics 74–76 (1998) 913–921.

[11] ACE, Active Control in Civil Engineering, EC Brite-Euram Contract N° BRPR-CT97-0402, 1997–2000.

[12] W. Pakos, The Experimental and Theoretical Analysis of Active Elimination of Cables Vibration in Cable Stayed Footbridges, (Ph.D. thesis), Politechnika Wrocławska, Wrocław, 2012 (in Polish).

[13] W. Pakos, Z. Wójcicki, Vibration control of a cable-stayed footbridge using the tension changes of cable, in: Proceedings in Applied Mathematics and Mechanics, Procedia Engineering 91 (2014) 142–147.

[14] Z. Wójcicki, W. Pakos, J. Grosel, W. Sawicki, Analytical and experimental dynamic studies of the cable-stayed bridge model, in: Polsko-Słowacko-Rosyjskie Seminarium, Teoretyczne podstawy budownictwa, 2011 (in Polish).

[15] J. Grosel, W. Sawicki, W. Pakos, Application of classical and operational modal analysis for examination of engineering structures, in: Proceedings in Applied Mathematics and Mechanics, Procedia Engineering 91 (2014) 136–141.

[16] Z. Wójcicki, J. Grosel, W. Sawicki, K. Majcher, W. Pakos, Experimental (OMA) and numerical (FEM) modal analysis of ball mill foundations, Procedia Engineering 111 (2015) 858–863.

[17] J. Grosel, W. Pakos, W. Sawicki, Experimental measurements as the basis for determination of the source of pumps' excessive vibration, Procedia Engineering 111 (2015) 269–276.

[18] H. Hossdorf, Statics of Modeling, Arkady, Warszawa, 1975 (in Polish).

[19] L. Müller, Dimensional Analysis Application in the Studies of Models, Biblioteka Naukowa Inżyniera, Warszawa, 1983 (in Polish).

[20] E. Buckingham, On physically similar systems: illustrations of the use of dimensional equations, Physical Review 4 (1914) 345–376.

[21] S. Ziemba, Vibration Analysis, PWN, Warszawa, 1957 (in Polish).

[22] H. Yamaguchi, I. Manabu, Mode-dependence of structural damping in cable-stayed bridges, Journal of Wind Engineering and Industrial Aerodynamics 72 (1997) 289–300.

[23] Z. Wójcicki, J. Grosel, Structural Dynamics, Wrocław University of Technology PRINTPAP, Wrocław Łódź, 2011 http://www.dbc.wroc.pl/publication/26131.

[24] K. Żółtowski, Pedestrian on Footbridge – Loads and the Response, Politechnika Gdańska, Gdańsk, 2007.